Macromolecules

ARTICLE

pubs.acs.org/Macromolecules

Synthesis and Analysis of Zwitterionic Spherical Polyelectrolyte Brushes in Aqueous Solution

Frank Polzer,[†,‡] Johannes Heigl,[†,‡] Christian Schneider,[†,‡] Matthias Ballauff,[*,†,‡] and Oleg V. Borisov[§,⊥]

[†]Helmholtz-Zentrum Berlin für Materialien und Energie GmbH, Hahn-Meitner-Platz 1, 14109 Berlin, Germany

[‡]Department of Physics, Humboldt University Berlin, Newtonstrasse 15, 12489 Berlin, Germany

[§]Institut Pluridisciplinaire de Recherche sur l'Environnement et les Matériaux, UMR 5254 CNRS/UPPA, Pau, France

[⊥]Institute of Macromolecular Compounds, Russian Academy of Sciences, 199004 St. Petersburg, Russia

Supporting Information

ABSTRACT: We present the synthesis and characterization of spherical polyelectrolyte brush (SPB) particles carrying zwitterionic polyelectrolyte chains. The colloidal particles consist of a divinylbenzene cross-linked poly(styrene) core (PS-*co*-DVB core) of about 100 nm in diameter onto which linear zwitterionic poly(2-(methacryloyloxy)ethyl dimethyl-(3-sulfopropyl)-ammonium hydroxide) (pMEDSAH) chains are chemically grafted via ATRP. ζ-Potential measurements demonstrated that the SPB has an electrophoretic mobility due to the net charge of the PS-*co*-DVB core particles. There is an increase of the brush thickness L of the zwitterionic brush at high concentrations of sodium chloride at room temperature. Temperature-dependent measurements by dynamic light scattering (DLS) showed that the zwitterionic SPBs swell reversibly with increasing temperature because of the upper critical solution temperature (UCST) of the pMEDSAH chains in water. This effect could be enhanced by the addition of salt. Cryogenic transmission electron microscopy (cryoTEM) showed that the shell of the particles is quite compact at room temperature. However, the hydrodynamic radius as measured by DLS was significantly larger than the particles radius inferred from microscopy. This result is explained in terms of a model in which the shell of the zwitterionic SPB undergoes a phase separation into a dense phase and a few chains sticking out into the aqueous phase.

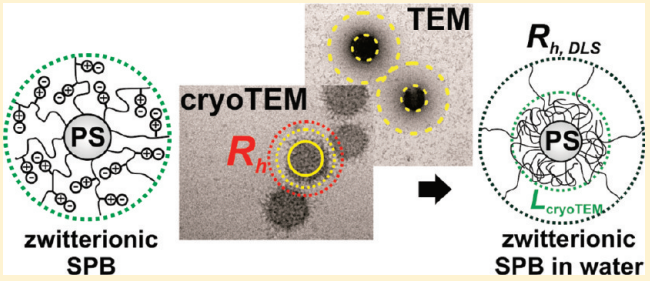

INTRODUCTION

Polyampholytes in general and specifically zwitterionic polymers have become of great importance in the last decades due to their possible applications.[1−3] This includes ultralow fouling coatings and high-tech applications as biocompatible components for drug delivery.[4−6] Colloidal polymer brushes in which the radius of gyration of the grafted polymer chains exceeds the average distance between the joints of the polymer chains can be prepared by surface polymerization of attached initiators (grafting-from).[7,8] Up to now, there have been a large number of studies devoted to noncharged and charged polymer brushes.[7,8] However, there exists much less work on zwitterionic polyelectrolyte brushes so far. To the authors' best knowledge, there are only a few studies of planar zwitterionic brushes: Azzaroni and co-workers successfully synthesized zwitterionic polymer brushes consisting of poly(2-(methacryloyloxy)ethyl dimethyl-(3-sulfopropyl)ammonium hydroxide) (pMEDSAH) by grafting-from bromide functionalized gold and silicon dioxide surfaces.[9] They observed hydrophilic and hydrophobic brush regimes depending on the height of the synthesized brush. In a further investigation they showed that one can tune the brush behavior by changing the temperature, which was explained by the upper critical solution temperature (UCST) of polysulfobetains.[10] Using atomic force microscopy and neutron reflectometry Terayama et al. showed that planar brushes made from poly(3-dimethyl(methacryloyloxyethyl)ammonium propane (pMPDSAH) swell by the addition of salt in aqueous solution.[11] The interaction of proteins with planar pMEDSAH and poly(1-carboxy-*N*,*N*-dimethyl-*N*-(2′-methacryloyloxyethyl) methanaminium inner salt) (pCBMA) brushes was thoroughly studied by Zhang and co-workers.[12] They observed that these systems possess a high resistance against nonspecific protein adsorption.[13] Moreover, planar brushes of poly(2-methacryloyloxyethyl phosphorylcholine) (pMPC) provide excellent lubrication in aqueous media which makes them promising candidates for applications as boundary lubricants in artificial joints or similar systems.[14,15]

All systems mentioned so far are planar systems. Since one of the most interesting properties of zwitterionic polymer brushes is their resistance against nonspecific protein adsorption and their biocompatibility, a promising field of application is drug delivery.[16−18] Therefore, these polyzwitterions were used as coatings for inorganic or organic nanoparticles and colloids such as

Received: December 23, 2010
Revised: January 25, 2011
Published: February 21, 2011

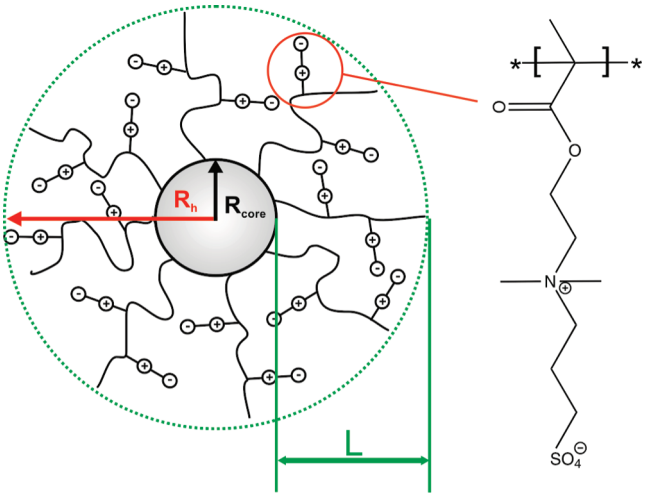

Figure 1. Schematic representation of the zwitterionic SPB with a PS-*co*-DVB/BIEM core and a shell of polysulfobetaine chains. The shell of the SPB consists of p[2-(Methacryloyloxy)ethyl dimethyl-(3-sulfopropyl)ammonium hydroxide] (pMEDSAH) which forms an inner salt. The brush thickness L is defined as the difference between the hydrodynamic radius of the core particles R_{core} and the R_h of the zwitterionic SPB particles.

gold, magnetite or silica nanoparticles, quantum dots, carbon nanotubes or even DNA.[19−24] However, the number of systematical studies investigating the solution behavior of zwitterionic SPB in aqueous medium is scarce. Matsuda et al. investigated the interactions of a zwitterionic SPB with a silica nanoparticle core and pMPC chains.[25] They observed no salt induced changes of the brush layer of the zwitterionic SPB investigated by dynamic light scattering (DLS). Since pMEDSAH possesses a UCST, temperature dependent measurements were conducted in previous investigations on planar carboxybetaine and sulfobetaine brushes.[26]

Here we present a comprehensive study of a zwitterionic spherical polyelectrolyte brush in aqueous solution. Figure 1 gives the structure of these particles in a schematic fashion. A shell of densely grafted p[2-(methacryloyloxy)ethyl dimethyl-(3-sulfopropyl)ammonium hydroxide] (pMEDSAH) has been affixed to nearly monodisperse core particles consisting of PS-co DVB and a thin surface layer of BIEM with a diameter of about 100 nm. Atom transfer radical polymerization (ATRP[27]) is used for grafting these polyzwitterionic chains to the surface. Since the core particles are practically monodisperse, the thickness of the brush layer can be easily monitored by DLS. Moreover, the particles can be studied by cryoTEM in the aqueous phase, that is, *in situ*. Special emphasis is laid on the dependence of the zwitterionic SPB on the salt concentration at different temperatures.

EXPERIMENTAL PART

Materials. All chemicals used in this study were of analytical grade. Styrene (Aldrich) was purified by column chromatography using inhibitor remover for 4-*tert*-butylcatechol (Aldrich) as column material. Copper(I) chloride (Aldrich), bipyridyl (bipy, Aldrich), potassium peroxodisulfate (KPS, Fluka), sodium dodecyl sulfate (SDS, Merck), cesium iodide (CsI, Aldrich) and (2-(methacryloyloxy)ethyl dimethyl-(3-sulfopropyl)ammonium hydroxide) (MEDSAH, Aldrich) were used as received. In this work, we always used 18 MΩ Millipore water.

Synthesis of BIEM. The synthesis of the vinyl-functionalized ATRP initiator 2-(2-bromoisobutyryloxy) ethyl methacrylate (BIEM) was conducted as reported previously.[28] In a typical run 28.3 g of 2-hydroxyethyl methacrylate (217 mmol) and 20 mL of pyridine (248 mmol) were dissolved in 200 mL of dichlormethane (DCM). The mixture was degassed by bubbling nitrogen to the solution and cooled down in an ice bath. A solution of 50 g (217 mmol) of 2-bromoisobutyryl bromide in 50 mL DCM was slowly added under nitrogen flow using a KDS 100 syringe pump (KD Scientific). The reaction was then stirred for 4 h. The precipitated product was filtered and purified by washing three times with 50 mL of water and dried over $MgSO_4$. Flash chromatography with mixtures of *n*-hexane/ethyl acetate with a ratio of 6:1 was conducted for purification. The successful synthesis of BIEM was proven by ^{1}H NMR in $CDCl_3$. The NMR spectrum can be found in the Supporting Information in Figure S1.

Synthesis of PS-*co*-DVB/BIEM Core−Shell Latex Particles. The core−shell latex particles were synthesized using a conventional emulsion polymerization under starved conditions as described recently.[29] For this purpose, 0.40 g (13.9 mmol) of SDS was dissolved in 250 mL of water under stirring. Subsequently, 20.16 g (0.19 mol) of styrene mixed with 1.30 g (1 mmol) of DVB was added. The polymerization was started by adding 0.30 g of KPS dissolved in 15 mL of water to the solution. The reaction was run at 80 °C for 1 h. Then, 2.70 g of BIEM dissolved in 7.30 g acetone was added under starved conditions at 70 °C with a dosage rate of 30 mL·h^{-1}. The addition of BIEM under starved conditions inhibits new particle formation and ensures the generation of a thin layer of BIEM on the surface of the PS-*co*-DVB core particles. After the addition was completed, the reaction was stirred at 70 °C for 7 h and then cooled down to room temperature. The dispersion was purified by ultrafiltration against a 10-fold excess of water.

Synthesis of Zwitterionic SPB. The synthesis of the zwitterionic SPB was conducted with an aqueous ATRP. A 15 g sample of a 1 wt % aqueous dispersion of PS-*co*-DVB/BIEM1 core−shell latex particles, 4.86 g (17.4 mmol) of MEDSAH, 0.5 g (3.2 mmol) of bipy, and 15 mL of water were placed in a flask equipped with a septum. The mixture was bubbled with nitrogen for 30 min to remove oxygen. Meanwhile 0.16 g (1.6 mmol) of CuCl and 0.26 g (3.5 mmol) of KCl were also degassed by nitrogen treatment in a second vessel equipped with a septum. The polymerization was started by the transfer of the aqueous dispersion to the CuCl/KCl mixture in a second vessel under vigorous stirring and oxygen exclusion via a cannula. The reaction was run at room temperature overnight and quenched by the exposition to air. The SPB dispersion was purified by dialysis against a 20-fold excess of water. For the analysis of the molecular weight of the grafted pMEDSAH chains, the SPB were put in 200 mL of 2 M NaOH. The reaction was heated to 100 °C for 10 days under reflux. After that, the mixture was cooled down to room temperature and neutralized with hydrochloric acid. The cleaved chains were separated from the core particles and cleaned by ultrafiltration. Aqueous gel permeation chromatography (GPC) with poly(methacrylic acid) (pMAA) calibration was used to determine the number-average molecular weight M_n and the molecular weight distribution *MWD*.

Methods. DLS was performed with an ALV 4000 (ALV GmbH, Langen, Germany) light scattering goniometer. Transmission electron microscopy (TEM) and cryogenic transmission electron microscopy (cryoTEM) measurements were conducted with a Zeiss EM922 EF-TEM (Zeiss NTS GmbH, Oberkochen, Germany) as described recently.[30] Some of the cryoTEM samples were mixed with CsI solution to increase the contrast of the shell. Therefore, the SPB dispersion was diluted with CsI solution to reach a solid content of 0.1 wt % of SPB and the desired concentration of CsI. The molar amount of sulfur of the SPB, and thus the core to shell ratio m_c/m_s, was determined by inductive-coupled plasma optical emission spectroscopy (ICP-OES) using a Varian Vista-Pro Radial (Agilent Technologies, Santa Clara, USA). Ion chromatography (IC) was used to determine the amount of bromine

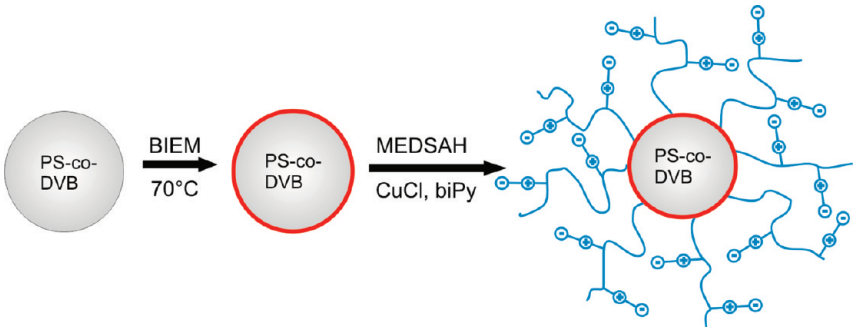

Figure 2. Scheme of the synthesis of zwitterionic SPB particles with pMEDSAH chains. In the first step, a PS-*co*-DVB latex particle is functionalized by the addition of ATRP initiator BIEM (red layer) in an emulsion polymerization under starved conditions. The pMEDSAH chains are covalently attached to the PS-*co*-DVB/BIEM particles via ATRP in aqueous solution.

on the PS-*co*-DVB/BIEM latex particles. ζ-Potential measurements were performed with a Malvern Zetasizer Nano ZS equipped with a 50 mW He−Ne−Laser using folded capillary cells with gold electrodes (Malvern Instruments, U.K.). The ζ-potentials were calculated out of the measured electrophoretic mobilities using the model of O'Brien and White.[31] For this, the software MPEK has been used.[32] Nuclear magnetic resonance spectroscopy (NMR) was conducted with a 250 MHz NMR (Bruker, Billerica, MA). The M_n and the polydispersity index (PDI) of the cleaved polymer chains of the brush layer were determined by aqueous GPC with a pMAA calibration.

RESULTS AND DISCUSSION

Synthesis of PS-*co*-DVB/BIEM Core−Shell Latex Particles. We synthesized two batches of BIEM functionalized latex particles via conventional emulsion polymerization. The reactions differ only in the amount of BIEM used. 9.7 mmol of BIEM were used for the synthesis of the system PS-*co*-DVB/BIEM1 whereas for PS-*co*-DVB/BIEM2 the amount was doubled to 19.4 mmol. The mass fraction of bromide according to IC was 2.3 ± 0.1 wt % for PS-*co*-DVB/BIEM1 and 4.5 ± 0.1 wt % for PS-*co*-DVB/BIEM2. These results show that the incorporation of the ATRP initiator BIEM is controlled by the amount of BIEM added to the emulsion polymerization. DLS measurements gave a hydrodynamic radius R_h of 48.1 ± 0.2 nm for the core particles PS-*co*-DVB/BIEM1 and 59.9 ± 0.2 nm for PS-*co*-DVB/BIEM2. The increase in R_h can only be explained by the higher amount of BIEM used for the synthesis of PS-*co*-DVB/BIEM2 since all other parameters were kept constant.[33] TEM micrographs for both systems presented in Figure S2 reveal monodisperse core particles of spherical shape. This was also recently found for emulsion polymerization under starved conditions using a polymerizable photoinitiator for surface functionalization.[34] Small-angle X-ray studies for this type of core−shell latex particles revealed a shell thickness of about 2 nm of the photoinitiator on the surface of the core−shell latex particles.[7] The synthesis of the zwitterionic SPB presented in this study was conducted using the core particles PS-*co*-DVB/BIEM1.

Synthesis of Zwitterionic SPB. A schematic representation of the complete synthesis of the zwitterionic SPB is given in Figure 2. The zwitterionic SPB with pMEDSAH chains were synthesized by aqueous ATRP using PS-*co*-DVB/BIEM1 core particles as the macroinitiator. The reactions were carried out under exclusion of oxygen to prevent oxidation of the catalyst $Cu^{I}Cl$. This could be easily recognized by the color of the bipy-CuCl complex formed in water. The Cu(I) complex was of brownish color whereas the Cu(II) complex was of turquoise color and results after quenching of the reaction mixture with air. After intensive purification by dialysis, the zwitterionic SPB was characterized by DLS measurements at room temperature which gave a R_h of 95.0 ± 2.2 nm. Thus, R_h increased about 47 nm due to the generation of the pMEDSAH shell as compared to the bare core particles. This increase of R_h is in the same range as reported for the shell synthesis via a free radical polymerization described for anionic and cationic SPBs.[34] The ratio m_c/m_s was determined to 2.06 ± 0.25 according to ICP-OES measurements of the sulfur content of the SPB. This value is higher than for SPBs prepared in earlier investigations by free radical photoemulsion polymerization. An explanation for this result is the higher molecular weight of the monomer used in this study. Furthermore, analysis of the cleaved polymer chains by GPC as displayed in Figure S3 (Supporting Information) revealed a M_n of about 60 000 $g \cdot mol^{-1}$ with a polydispersity index of 1.16. The determination of absolute molecular weights by aqueous GPC using a pMAA calibration should be discussed with caution. Compared to SPBs generated by photoemulsion polymerization, the PDI is about two times lower.[34] This is due to the use of a controlled living radical polymerization instead of a free radical polymerization. A PDI of 1.16 is a satisfactory result for aqueous ATRP considering the fact that water-based ATRP is a fast polymerization process and therefore difficult to control.[35] The grafting density was calculated to be 0.08 ± 0.01 nm^{-2} based on R_{core}, m_c/m_s and the degree of polymerization DP of the polymer chains in the shell. This grafting density is in the same order of magnitude as found for the grafting-from process using latex spheres as macroinitiators.[36] The value verifies that the generated zwitterionic core shell particles are within the limits of a spherical polymer brush.

ζ-Potential measurements have been conducted to elucidate the net charge of the particles. In principle, the pMEDSAH brush particles should exhibit charge neutrality due to their zwitterionic nature. Therefore, the ζ-potential should be zero. However, electrophoretic mobility measurements of the zwitterionic SPB as a function of the KCl concentration reveal a negative ζ-potential, as shown in Figure 3. Mary et al. also observed negative ζ-potentials for linear pMEDSAH chains in their study.[26] The authors explained this effect by a partial hydrolysis of the ester bond of the side chain of MEDSAH during the synthesis of the polymer. This leads to a statistical random copolymer of pMEDSAH and pMAA which was proven by NMR spectroscopy. Since pMAA is partially deprotonated a negative excess charge is

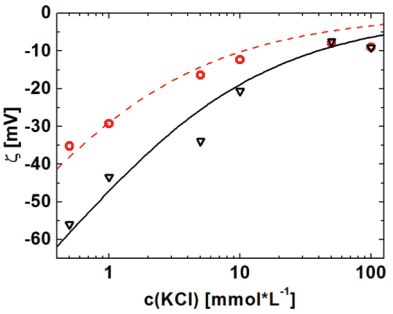

Figure 3. Measurements of the ζ-potential of the zwitterionic SPB with pMEDSAH chains (red ○) and of the bare PS-*co*-DVB/BIEM latex particles (▽) in dependence of the concentration of KCl. The lines show the best fit results of the ζ-potential data for both systems using eq 1 with a constant particle charge. The data points for the SPB and the bare core particles fall together at the two highest salt concentrations.

observed in aqueous solution. However, the particle synthesis presented here is performed in neutral medium so that hydrolysis of the chains is negligible small.

To investigate the negative ζ-potential of the zwitterionic SPB particles in more detail, electrophoretic mobility experiments as a function of the KCl concentration were performed using the core particles before the grafting of the zwitterionic shell. The results are plotted in Figure 3. Here a negative ζ-potential is observed as well which decreases toward zero with increasing salt content. The negative charge is due to KPS and anionic surfactant residues incorporated during the synthesis of the core particles which are present even after extensive cleaning.

The relation of the ζ-potential to the surface charge as a function of the salt concentration for homogeneous spheres with an electrokinetic charge Q_{ek} is given by[37]

$$Q_{ek} = \frac{2R_h(1 + R_h\kappa)}{l_B} \sin\left(\frac{ez\zeta}{2k_BT}\right) \qquad (1)$$

where κ is the inverse Debye length, l_B is the Bjerrum length, e is the charge of an electron, z is the valence of the counterions and k_BT is the thermal energy. Eq 1 can be used to fit the experimental data of the ζ-potential where Q_{ek} is the only fitting parameter.[38] Furthermore, Q_{ek} is assumed to be constant and independent of the salt concentration. The respective fits are shown in Figure 3 (solid and broken lines). For both, the bare core and the SPB particles, good fits over 3 orders of magnitude in salt concentration could be achieved. The resulting electrokinetic charge densities are $-2 \cdot 10^{-2}$ C·m^{-2} for the core particles and $-1 \cdot 10^{-2}$ C·m^{-2} for the zwitterionic SPBs, respectively. Since the charge density of the SPB particles is smaller than the charge on the bare particles, there can be no additional contribution of any negative charges arising from the zwitterionic shell. Therefore, we conclude that the ζ-potential of the zwitterionic SPBs is caused by the negative excess charges located on the surface of the core particles.

We now turn to the discussion of the TEM micrographs of the zwitterionic SPB. The contrast of the pMEDSAH shell of the particles was increased by adding CsI to the dispersion. This is due to the fact that both the Cs^+-ion and the I^--ion act as counterions in the shell which improves the electron contrast considerably (Figure 4). The PS-*co*-DVB/BIEM core particles are visible as dark spherical objects with a characteristic size of about 100 nm in diameter. This size is in good agreement with DLS measurements of the bare core particles. Figure 4a also shows spherical shaped shells around each core particle due to the grafted pMEDSAH chains, which are marked with yellow dotted circles. Measurements of the shell thickness in the dried state according to the TEM micrographs reveal values of about 110 nm resulting in an overall radius of the SPB of about 160 nm. The chains of the shell are fully stretched when the particles are immobilized on a TEM grid. This indicates an attractive interaction of the zwitterionic chains with the carbon support (Figure 4c). The effect is due to the pretreatment of the grids by a glim charge which generates negative surface charges on the support film and thus makes the support more hydrophilic. The surface charge of the carbon film then interacts with the charges of the pMEDSAH chains.[39]

Compared to the hydrodynamic shell thickness L of the dispersed zwitterionic SPB there is a discrepancy to the TEM shell thickness in the dried state of about 60 nm. This finding can be explained by the fact that the shell is not in a fully stretched state when the SPB particles are dispersed in water. The difference of the TEM images in which a fully stretched state is visible and the results from DLS measurements points out that the shell is in a collapsed state in aqueous solution.

To obtain detailed microscopic information on the zwitterionic SPB in aqueous solution, cryoTEM measurements have been conducted.[40,41] Figure 5 shows cryoTEM micrographs of the zwitterionic system dispersed in salt-free solution and in 0.1 M CsI solutions. Figure 5a shows the dispersed zwitterionic SPB in nonsaline environment. The radius of the particles increased compared to the radius of the bare core particles. Additionally, the surface of the SPB is corrugated because of the pMEDSAH shell on the core particles. Vitrifying the particles in 0.1 M CsI solution leads to a significant increase in the electron density of the shell as it can be seen in the cryoTEM micrographs in Figure 5b. In this way the shell can be visualized in a much better way. However, subsequent DLS data (see the discussion of Figure 7 below) demonstrates that the addition of salt in this concentration regime does not alter the conformation of the shell.

In Figure 5b the pMEDSAH chains of the shell are clearly visible due to the presence of CsI. The radius of the particles is about 80 nm. Figure 5b demonstrates that a closed shell of pMEDSAH is grafted onto the PS-*co*-DVB/BIEM core−shell latex particles. That directly proves that a closed shell of BIEM has been generated by the emulsion polymerization under starved conditions which is in agreement with past studies.[7] The deviation between the results for L and the shell thickness observed by cryoTEM gives important information about the conformation of the pMEDSAH shell of the zwitterionic SPB. The cryoTEM images show a shell thickness of pMEDSAH chains of about 32 nm, whereas L obtained by DLS is about 48 nm. The fact that the shell thickness according to cryoTEM and DLS differs can be explained by the fact that in light scattering the particle size is determined by the longest chains of the SPB.[42] The longest or most stretched pMEDSAH chains are not visible in the cryoTEM images because of the poor contrast of single polymer chains even after introducing CsI to the solution.

This leads us to the conclusion that the zwitterionic shell of the SPB is not fully stretched in the dispersed state. Most of the chains are collapsed so that a layer of about 40 nm thickness results. Only a few chains stretch further away from the core and thus cause the measured L in the DLS experiment. This behavior is schematically depicted in Figure 6 and is in qualitative

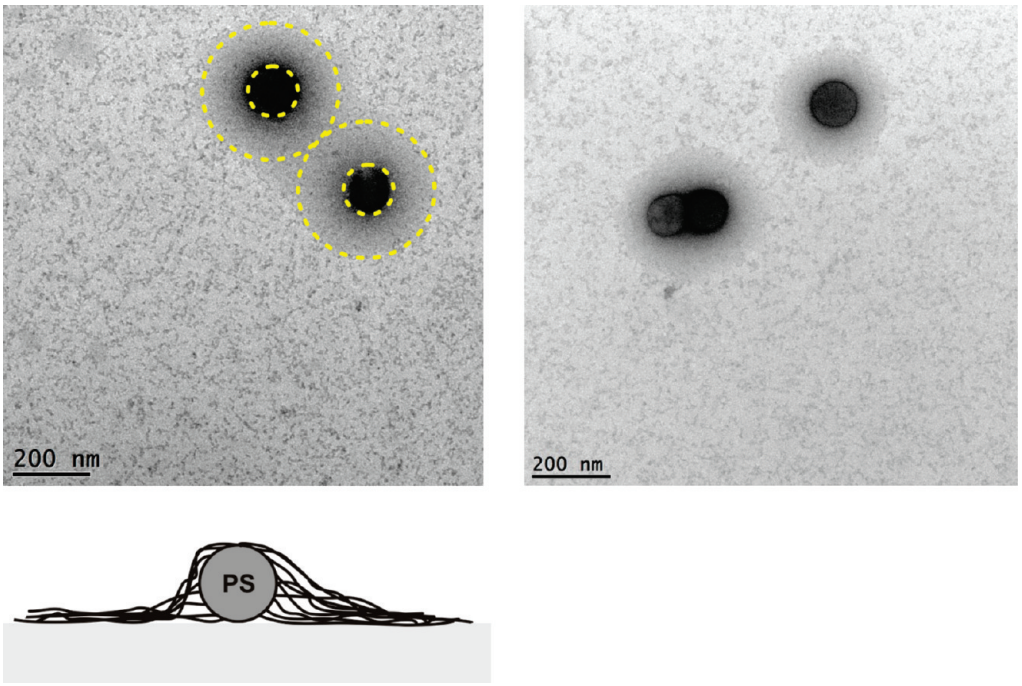

Figure 4. TEM micrographs of the zwitterionic SPB prepared on a carbon support. A 0.1 M CsI solution has been used to enhance the contrast of the shell. The lower part displays the structure of the particles on the surface in a schematic fashion.

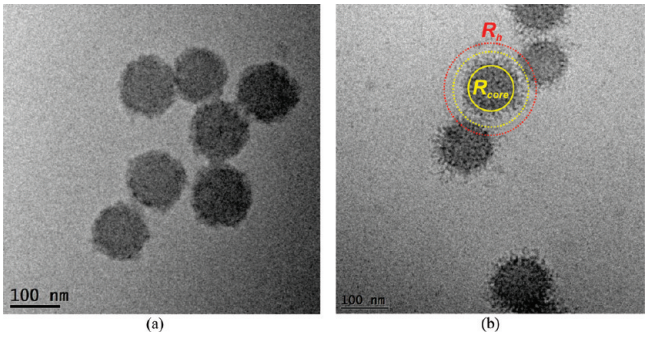

Figure 5. CryoTEM micrographs of the zwitterionic SPB in aqueous solution without any salt (a) and in 0.1 M CsI solution (b). Figure 5b includes hydrodynamic radii of the bare core particles R_{core} and of the core−shell particles R_h as determined by DLS.

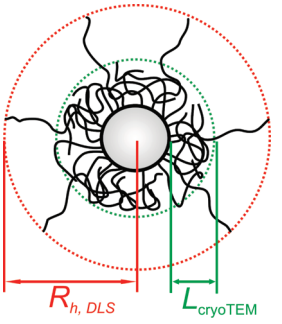

Figure 6. Model for the zwitterionic SPB in aqueous solution. In a poor solvent, e.g. in water, most of the chains are in a collapsed state. Only a small portion of the chains is stretched further away into solution. This fact is revealed by comparing the shell thickness observed in cryoTEM micrographs with the results for L determined by DLS. Thus, the shell of the zwitterionic SPB undergoes a phase separation into a condensed phase near the surface of the core particles and a dilute swollen layer of the shell which extends far into the solution.

agreement with the model derived from Wagner et al.[43] These authors considered a collapse transition in a polymer brush caused by formation of clusters comprising $n \geq 3$ monomer groups.[43] In our case, we can expect association of $n \geq 3$ dipole groups inside the brush into stable clusters. Furthermore, the formation of stable clusters can also be induced by hydrophobic interactions of the polymer backbone of the pMEDSAH chains. Both effects lead to a collapse transition accompanied by the microphase segregation inside the brush: A dense phase is formed close to the grafting surface whereas the sparse periphery of the brush is formed by more extended chains. Thus, this phase separation causes a bimodal distribution of the polymer chains with respect to their extension. A similar trend has also been predicted for the complexation of polymer brushes with surfactants.[44] In the present case, water represents the poor solvent for the pMEDSAH chains, which leads to a collapse of the shell polymer.[45] A part of the pMEDSAH chains is not included in the surface-near layer leading to an internal phase separation which causes a lateral inhomogeneity. The chains in the dilute swollen layer of the shell extend further out into the solution and cause a significant contribution to L in the DLS experiments.

Since in the model shown in Figure 6 the majority of the pMEDSAH chains are in a collapsed state, investigations have been conducted to elucidate if this structure can be influenced by external stimuli. Therefore, DLS measurements of the core−shell particles at different concentrations of NaCl have been done. Figure 7 shows the results of the salt-dependent measurements. There is no notable increase in L of the zwitterionic SPB within the limits of error upon salt addition up to concentrations of 0.5 mol·L^{-1}. These results are in good agreement with those of Matsuda and co-workers who also did not observe a swelling of

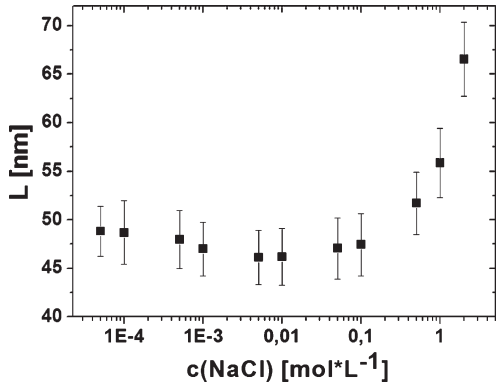

Figure 7. Salt dependent measurements of L of the zwitterionic SPB via DLS at a temperature of 25 °C. The pMEDSAH shell shows a swelling of L at concentrations of NaCl higher than 0.5 mol·L^{-1}.

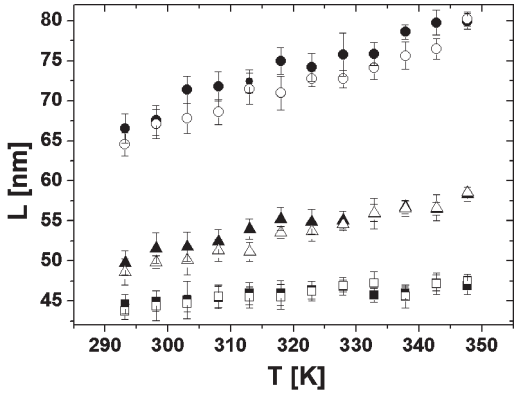

Figure 8. Temperature dependent measurements of L of the zwitterionic SPB with pMEDSAH chains by DLS. Increasing the temperature from 20 to 75 °C leads to a swelling of the brush layer of the zwitterionic SPB. The behavior is completely reversible, which was shown by subsequent cooling of the system. Therefore, it can be assigned to the UCST of the pMEDSAH chains. The effect of swelling can be significantly enhanced by the addition of high amounts of salt. The lowest data set represents a heating cycle of the zwitterionic SPB in salt-free solution (■ heating and □ cooling), the second curve shows the swelling of the zwitterionic SPB in 1 mol·L^{-1} NaCl solution (▲ heating and Δ cooling) and 2 mol·L^{-1} NaCl solution for the uppermost curve (● heating and ○ cooling).

the zwitterionic pMPC shell upon the addition of up to 0.5 mol·L^{-1} salt.[25] They conclude that the chains are already fully extended even in nonsaline solution due to the excluded volume effect of densely packed polymer chains in polymer brushes. However, Figure 7 indicates an increase of L starting at salt concentrations higher than 0.5 mol·L^{-1}, which results in a 40% higher L at 2 mol·L^{-1} as compared to the nonsaline state. The increase in L shows that the SPB shell is not fully extended in the nonsaline state, which is in full accordance with the model proposed in Figure 6.

Figure 7 demonstrates that the solution behavior of the pMEDSAH chains is changed, if the salt concentration is sufficiently high. The observation that the onset of the swelling of the shell takes place at concentrations higher than 0.5 mol·L^{-1} indicates that the swelling cannot be related to the conventional antipolyelectrolyte effect. The antipolyelectrolyte effect is generally understood as a Coulomb screening effect which is typically observed for salt concentration up to 0.01 mol·L^{-1}.[46] The response of the pMEDSAH shell at salt concentrations higher than 0.5 mol·L^{-1} suggests that ion-specific and hydrophobic interactions may play a role in these systems.[47] An alternative explanation may be sought in the breaking of salt bridges in the zwitterionic layer that occurs only at high salt concentrations.[48]

We now turn to the investigations of the temperature-dependent behavior of the zwitterionic SPB. Figure 8 demonstrates that there is an increase in L of about 7 nm upon heating. The results for the cooling and reheating fully agree and show a good reproducibility. The stretching of the shell at high temperatures is due to the UCST behavior of the pMEDSAH chains. At higher temperatures, the solvent quality will increase for pMEDSAH chains due to their UCST temperature. This has been found by different groups in earlier works on planar brushes.[9,10] In the system under consideration here, the expansion of the shell is not very pronounced as compared to the salt-dependent measurements presented in Figure 7. Since the results of the previous paragraph showed that the addition of high amounts of salt significantly increased L at room temperature, temperature-dependent DLS measurements at different salt concentrations have been conducted.

The results of these measurements are also presented in Figure 8 and show two important effects: On the one hand, L significantly increases at room temperature at salt concentrations higher than 1 mol·L^{-1}. This finding has been shown earlier in Figure 7. Additionally, temperature cycles at different salt concentrations reveal a drastic swelling of the zwitterionic shell upon heating. This is due to the increase of the solvent quality for the zwitterionic polymer chains. The UCST behavior gets more pronounced after the addition of salt which was expected since both, the salt concentrations and the temperature, are increasing the solubility of the pMEDSAH chains. The influence of the amount of added salt onto the UCST of pMEDSAH homopolymer was also observed by Mary et al.[26]

■ CONCLUSION

We presented a method for the synthesis of colloidal stable spherical polymer brushes with a zwitterionic brush layer of pMEDSAH chains. The extension of the shell can be influenced upon the addition of salt which may be due to ion-specific interactions. Furthermore, the zwitterionic shell showed a fully reversible swelling upon heating due to the UCST behavior of the pMEDSAH chains. This effect could be enhanced upon the addition of salt. By a combination of DLS, TEM and cryoTEM measurements we propose a model for the zwitterionic SPB including an internal phase separation of the pMEDSAH shell according to Wagner et al.[43] In this model, the shell is mostly collapsed in a condensed state near the surface of the core particles whereas only a small portion of the shell is in a dilute swollen state with the pMEDSAH chains extending far out into solution.

■ ASSOCIATED CONTENT

Supporting Information. ^{1}H NMR of BIEM, TEM micrographs of PS-*co*-BIEM1 and PS-*co*-DVB-*co*-BIEM2 core particles, and GPC curve of the cleaved chains of the brush polymer. This material is available free of charge via the Internet at http://pubs.acs.org.

AUTHOR INFORMATION

Corresponding Author
*E-mail: Matthias.Ballauff@helmholtz-berlin.de.

ACKNOWLEDGMENT

We thank the Deutsche Forschungsgemeinschaft, Sonderforschungsbereich 840 Bayreuth. C.S. thanks the Elite Study Program Macromolecular Science in the Elite Network Bavaria and the Bavarian Graduate Support Program for financial support. We thank R. Hill for the extensive support provided for using the MPEK software and J. Dzubiella for helpful discussions.

REFERENCES

(1) Kudaibergenov, S. E.; Cifferi, A. *Macromol. Rapid Comm.* **2007**, *28*, 1969–1986.
(2) Kudaibergenov, S. E.; Jaeger, W.; Laschewsky, A. *Adv. Polym. Sci.* **2006**, *201*, 157–224.
(3) Das, M.; Sanson, N.; Kumacheva, E. *Chem. Rev.* **2008**, *20*, 7157–7163.
(4) Zhang, Z.; Finlay, J. A.; Wang, L.; Gao, Y.; Callow, J. A.; Callow, M. E.; Jinag, S. *Langmuir* **2009**, *25*, 13516–13521.
(5) Matsuno, R.; Ishihara, K. *Macromol. Symp.* **2009**, *279*, 125–131.
(6) Cho, A. K.; Kong, B.; Choi, I. S. *Langmuir* **2007**, *23*, 5678–5682.
(7) Ballauff, M. *Prog. Polym. Sci.* **2007**, *32*, 1135–1151.
(8) Advincula, R. C.; Brittain, W. J.; Caster, K. C.; Rühe, J. editors *Polymer Brushes*; Wiley-VCH: Weinheim, Germany, 2005.
(9) Azaroni, O.; Brown, A. A.; Huck, W. T. S. *Angew. Chem.* **2006**, *118*, 1802–1806.
(10) Cheng, N.; Brown, A. A.; Azaroni, O.; Huck, W. T. S. *Macromolecules* **2008**, *41*, 6317–6321.
(11) Terayama, Y.; Kikuchi, M.; Kobayashi, M.; Hino, M.; Takahara, A. *J. Phys: Conf. Ser.* **2009**, *184*, 012011.
(12) Zhang, Z.; Chao, T.; Chen, S.; Jiang, S. *Langmuir* **2006**, *22*, 10072–10077.
(13) Ladd, J.; Zhang, Z.; Chen, S.; Hower, J. C.; Jiang, S. *Biomacromolecules* **2008**, *9*, 1357–1361.
(14) Chen, M.; Briscoe, W. H.; Armes, S. P.; Klein, J. *Science* **2009**, *323*, 1698–1701.
(15) Kobayashi, M.; Terayama, Y.; Hosaka, N.; Kaido, M.; Suzuki, A.; Yamada, N.; Torikai, N.; Ishihara, K.; Takahara, A. *Soft Matter* **2007**, *3*, 740–746.
(16) Li, G.; Xue, H.; Gao, C.; Zhang, F.; Jiang, S. *Macromolecules* **2010**, *43*, 14–16.
(17) Lobb, E.; Ma, I.; Billingham, N. C.; Lewis, A. L.; Armes, S. P. *J. Am. Chem. Soc.* **2001**, *123*, 7913–7914.
(18) Matsuura, K.; Ohno, K.; Kagaya, S.; Kitano, H. *Macromol. Chem. Phys.* **2007**, *208*, 862–873.
(19) Yuan, J. J.; Schmid, A.; Armes, S. P. *Langmuir* **2006**, *22*, 10022–10027.
(20) Yuan, J. J.; Armes, S. P.; Takabayashi, Y.; Prassides, K.; Leite, C. A. P.; Galembeck, F.; Lewis, A. L. M.; Schmid, A. *Langmuir* **2006**, *22*, 10989–10993.
(21) Yokohama, R.; Suzuki, S.; Shirai, K.; Yamauchi, T.; Tsubokawa, N.; Tsuchimochi, M. *Eur. Polym. J.* **2006**, *42*, 3221–3229.
(22) Matsuno, R.; Goto, Y.; Konno, T.; Takai, M.; Ishihara, K. *J. Nanosci. Nanotech.* **2009**, *9*, 358–365.
(23) Narain, R.; Housni, A.; Lane, L. *J. Polym. Sci., Part A* **2006**, *44*, 6558–6568.
(24) Giacomelli, C.; LeMen, L.; Borsali, R.; Him, J. L.-K.; Brisson, A.; Armes, S. P. *Biomacromolecules* **2006**, *7*, 817–828.
(25) Matsuda, Y.; Kobayashi, M.; Annaka, M.; Ishihara, K.; Takahara, A. *Langmuir* **2008**, *24*, 8772–8778.
(26) Mary, P.; Bendejacq, D. D.; Labeau, M.-P.; Dupuis, P. *J. Phys. Chem. B* **2007**, *27*, 7767–7777.
(27) Qiu, J.; Charleux, B.; Matyjaszewski, K. *Prog. Polym. Sci.* **2001**, *26*, 2083–2134.
(28) Podwika, M.; Gaynor, G. S.; Kulfan, A.; Matyjaszewski, K. *Macromolecules* **1997**, *30*, 5192–5194.
(29) Zhang, M.; Liu, L.; Zhao, H.; Yang, Y.; Fu, G.; He, B. *J. Colloid Interface Sci.* **2006**, *301*, 85–91.
(30) Crassous, J. J.; Rochette, C. N.; Wittemann, A.; Schrinner, M.; Drechsler, M.; Ballauff, M. *Langmuir* **2009**, *25*, 7862–7871.
(31) O'Brien, R. W.; White, L. R. J. *Chem. Soc. Faraday Trans II* **1978**, *2*, 1607–1626.
(32) The manual for the MPEK-software package can be downloaded from: Reghan, J. H. http://people.mcgill.ca/files/reghan.hill/MPEK-0.02.pdf
(33) Song, J.-S.; Winnik, M. A. *Macromolecules* **1995**, *38*, 8300–8307.
(34) Guo, X.; Ballauff, M. *Langmuir* **2000**, *16*, 8719–8726.
(35) Qiu, J.; Charleux, B.; Matyjaszewski, K. *Prog. Polym. Sci.* **2001**, *26*, 2083–2134.
(36) Schrinner, M.; Haupt, B.; Wittemann, A. *Chem. Eng. J.* **2008**, *144*, 138–145.
(37) Hanus, L. H.; Hartzler, R. U.; Wagner, N. J. *Langmuir* **2001**, *17*, 3136–3147.
(38) Hoffmann, M.; Jusufi, A.; Schneider, C.; Ballauff, M. *J. Colloid Interface Sci.* **2009**, *338*, 566–572.
(39) Mei, Y.; Wittemann, A.; Sharma, G.; Koch, T.; Gliemann, H.; Horbach, J.; Schimmel, T.; Ballauff, M. *Macromolecules* **2003**, *36*, 3452–3456.
(40) Crassous, J. J.; Wittemann, A.; Siebenbürger, M.; Schrinner, M.; Drechsler, M.; Ballauff, M. *J. Colloid Interface Sci.* **2008**, *286*, 805–812.
(41) Lu, Y.; Mei, Y.; Drechsler, M.; Ballauff, M. *J. Chem. Phys. B.* **2006**, *110*, 3930–3937.
(42) Samokhina, L.; Schrinner, M.; Ballauff, M. *Langmuir* **2007**, *23*, 3615–3619.
(43) Wagner, M.; Brochard-Wyart, F.; Hervet, H.; de Gennes, P.-G. *Colloid Polym. Sci.* **1993**, *271*, 621–628.
(44) Currie, E. P. K.; Fleer, G. J.; Cohen Stuart, M. A.; Borisov, O. *Eur. Phys. J. E* **2000**, *1*, 27–40.
(45) Bektrouv, E. A.; Kudaibergenov, S. E.; Rafikov, S. R. *Macromol. Chem. Phys.* **1990**, *C30*, 233–240.
(46) Salamone, J. C.; Tsai, C. C.; Watterson, A. C.; Olsen, A. P. *Polymer* **1978**, *19*, 1157–1162.
(47) Mary, P.; Bendejacq, D. D. *J. Phys. Chem. B.* **2008**, *112*, 2299–2310.
(48) Kabanov, V. A. Multilayer thin films. In *Sequential assembly of nanocomposite materials*; Decher, G.; Schlenoff, J. eds., Wiley-VCH: Weinheim, Germany, 2002.